


## Participation of MicroRNA-34a and RANKL on bone repair induced by poly(vinylidene-trifluoroethylene)/barium titanate membrane

Helena B. Lopes<sup>a\*</sup>, Emanuela P. Ferraz<sup>a</sup>, Adriana L. G. Almeida<sup>a</sup>, Pedro Florio<sup>a</sup>,  
Rossano Gimenes<sup>b</sup>, Adalberto L. Rosa<sup>a</sup> and Marcio M. Beloti<sup>a</sup> 

<sup>a</sup>Cell Culture Laboratory, School of Dentistry of Ribeirão Preto, University of São Paulo, Ribeirão Preto, Brazil;

<sup>b</sup>Institute of Physics and Chemistry, Federal University of Itajubá, Itajubá, Brazil

### ABSTRACT

The poly(vinylidene-trifluoroethylene)/barium titanate (PVDF) membrane enhances *in vitro* osteoblast differentiation and *in vivo* bone repair. Here, we hypothesized that this higher bone repair could be also due to bone resorption inhibition mediated by a microRNA (miR)/RANKL circuit. To test our hypothesis, the large-scale miR expression of bone tissue grown on PVDF and polytetrafluoroethylene (PTFE) membranes was evaluated to identify potential RANKL-targeted miRs modulated by PVDF. The animal model used was rat calvarial defects implanted with either PVDF or PTFE. At 4 and 8 weeks, the bone tissue grown on membranes was submitted to a large-scale analysis of miRs by microarray. The expression of miR-34a and some of its targets, including RANKL, were evaluated by real-time polymerase chain reaction and osteoclast activity was detected by tartrate-resistant acid phosphatase (TRAP) staining. Among more than 250 miRs, twelve, including miR-34a, were simultaneously higher expressed ( $\geq 2$  fold) at 4 and 8 weeks on PVDF. The higher expression of miR-34a was concomitant with a reduced expression of all its evaluated targets, including RANKL. Additionally, more TRAP-positive cells were observed in bone tissue grown on PTFE compared with PVDF in both time points. In conclusion, our results suggest that the higher bone formation induced by PVDF could be, at least in part, triggered by a miR-34a increase and RANKL decrease, which may inhibit osteoclast differentiation and activity, and bone resorption.

### ARTICLE HISTORY

Received 17 March 2016

Accepted 15 June 2016

### KEYWORDS

Bone; biomaterial; microRNA; osteoclast; RANKL

## 1. Introduction

The technique of guided bone regeneration is based on the use of barrier membranes to prevent soft tissue ingrowth and has been extensively used in dentistry to alveolar ridge augmentation and to repair bone defects.[1–3] A plethora of biomaterials has been developed to produce membranes with experimental and clinical promising results.[4–8]

Among the new biomaterials, the poly(vinylidene-trifluoroethylene)/barium titanate composite (PVDF) emerges as an alternative to guide bone formation.[9] Previous studies

**CONTACT** Marcio M. Beloti  [mmbeloti@usp.br](mailto:mmbeloti@usp.br)

\*Helena Bacha Lopes and Emanuela Prado Ferraz contributed equally to this work.

of our group showed that the PVDF membrane exhibits a higher *in vitro* biocompatibility compared with the polytetra-fluoroethylene (PTFE) membrane, the gold standard material for clinical applications.[10–12] We observed that PVDF membrane favors the adhesion and differentiation of human osteoblasts and periodontal ligament fibroblasts.[10–12] We also noticed a higher bone repair in rat calvarial bone defects treated with PVDF compared with PTFE 8 weeks post-implantation.[13] Interestingly, the receptor activator of nuclear factor kappa-B ligand (RANKL) expression of cells derived from the new bone tissue grown on PVDF was reduced compared with PTFE membrane.[13]

Bone repair is a complex process involving the differentiation and crosstalk of several cell types to regulate the balance between tissue formation and resorption that is tightly coordinated by local and systemic factors, such as receptor activator of nuclear factor kappa-B (RANK), RANKL, and osteoprotegerin (OPG).[14] Osteoblasts express RANKL that binds RANK on the osteoclast surface, triggering a crucial signal for osteoclast differentiation and, consequently, bone resorption.[15] This cell signaling may be modulated by OPG that binds RANKL preventing its interaction with RANK.[16]

The RANKL-mediated osteoclast formation is regulated by multiple transcriptional and post-transcriptional mechanisms including microRNAs (miRs). The miRs are endogenous, noncoding RNAs involved in mRNA cleavage or translational repression.[17] Although little is known about the effects of individual miRs on bone remodeling, several miRs play important roles in osteoclast differentiation such as miR-29b, -34a -124, -148a, and -155.[18–24]

Considering the relevance of miRs to the process of bone remodeling, we hypothesized that the higher bone repair induced by PVDF compared with PTFE membrane is also due to a decrease in bone resorption mediated by a miR/RANKL circuit. Therefore, here we evaluated the large-scale miR expression of the bone tissue grown on PVDF and PTFE membranes to identify potential RANKL-targeted miRs modulated by PVDF.

## **2. Materials and methods**

### **2.1. Membrane preparation**

Discs of PVDF membrane with 6 mm in diameter were prepared and characterized as previously described and commercially available PTFE membrane was used as control.[9,13]

### **2.2. Surgical procedure**

The surgical procedure for membrane implantation was performed as previously described under approval of the Committee of Ethics in Animal Research of the University of São Paulo.[13,25] Briefly, 16 Wistar rats weighting 200–250 g were anesthetized with ketamine (75 mg/kg body weight) (Agener União, SP, Brazil) and xylazine (6 mg/kg body weight) (Calier, MG, Brazil). An incision was made in the scalp along the sagittal suture to expose the parietal bones and one calvarial defect with 5 mm in diameter was created with a trephine bur (Neodent, PR, Brazil). Defects were randomly implanted with either PVDF or PTFE membrane ( $n = 8$ ). At the end of 4 and 8 weeks, the animals were euthanized, the calvarias harvested and processed for gene expression analyses and tartrate-resistant acid phosphatase (TRAP) staining.

### **2.3. Extraction and isolation of RNA**

Bone fragments of four different samples of either PVDF or PTFE membranes at 4 and 8 weeks were pooled, crushed and the total RNA was extracted with Trizol reagent (Gibco-Invitrogen, NY, USA) and isolated according to the manufacturer's instructions (chloroform-isopropanol). The quality of the total RNA was assessed using the Agilent 2100 Bioanalyzer (Agilent, CA, USA) and 5 µg of the total RNA was used for miR sequencing.

### **2.4. Microarray for miR detection**

After DNase (Gibco-Invitrogen) treatment, samples were submitted to miR sequencing at the Illumina HiSeq2000 (Illumina, CA, USA) using the latest versions of the sequencing reagents and flow cells providing up to 300 Gb of sequence information per flow cell. The TruSeq library generation kits were used following the manufacturer's instructions (Illumina). Library construction consists of random fragmentation of miR followed by complementary DNA (cDNA) production using random primers. The ends of the cDNA were repaired and A-tailed and adaptors ligated for indexing (up to 12 different barcodes per lane) during the sequencing runs. The cDNA libraries were quantified using quantitative Polymerase Chain Reaction (PCR) in a Roche LightCycler 480 with the Kapa Biosystems kit (Kapa Biosystems, MA, USA) prior to cluster generation. Clusters were generated to yield approximately 725–825 K clusters/mm<sup>2</sup>. Cluster density and quality were determined during the run. They run paired end 2 × 50 bp sequencing runs to align the cDNA sequences to the reference genome. Before alignment, the data were converted to the FASTQ Sanger format using FASTQ Groomer. TopHat was used to align RNA-Seq reads to the reference genome using the short read aligner Bowtie and to analyze the mapping results to identify splice junctions between exons. Cufflinks were used to align reads from TopHat to assemble transcripts, to estimate their abundances, and to test for differential expression and regulation. Cuffcompare, which is part of Cufflinks, compared the assembled transcripts to a reference annotation and tracked Cufflinks transcripts across multiple experiments. Finally, Cuffdiff indicated significant changes in miR transcript expression. The BAM file generated by TopHat was filtered and the read paired and mapped. A pileup from this filtered file with calling the consensus according to the MAQ model was created and this pileup filtered to report variants as well as to convert coordinates to intervals that were covered by a specified number of reads with bases above a set quality threshold. A total of 276 miRs were evaluated at 4 and 8 weeks and the data were compared using bioinformatics tools and only miRs with fold change  $\geq 2$  (increase or decrease),  $p$ -value  $< 0.05$  and  $q$ -value  $< 0.05$  were considered. To confirm the results of the miR sequencing, miR-146b at 4 weeks and miR-29b and -10a at 8 weeks were selected for validation by real-time PCR as described below. Additionally, the miR-34a expression was also evaluated by real-time PCR as it exerts a key role in the process of osteoclastogenesis.[24]

### **2.5. Real-time PCR**

The cDNA was synthesized using 1 µg of the RNA through a reverse transcription reaction (Promega Corporation, WI, USA). Real-time PCR was carried out in a CFX96 Real-Time PCR Detection System (Bio-Rad Laboratories, PA, USA) using 5 µL of TaqMan Universal

PCR Master Mix-No AmpErase UNG 2X (Gibco-Invitrogen), 0.5  $\mu$ L of TaqMan probes (20X TaqMan Gene Expression Assay Mix), and 11.25  $\mu$ g/ $\mu$ L of cDNA. It was evaluated the expression of miR-146b at 4 weeks and miR-29b and -10a at 8 weeks to validate the miR sequencing data. Also, the expression of miR-34a, a regulator of osteoclastogenesis, and some of its targets, RANKL, lymphoid enhancer-binding factor 1 (LEF1), endoglin (ENG), YY1 transcription factor (YY1), synaptotagmin 1 (SYT1), and colony-stimulating factor 1 receptor (CSFR) were evaluated.[24] The relative expression was normalized by constitutive genes (U6 for miRs and GAPDH for miR-34a targets) and the changes were relative to the expression of the bone tissue grown on PTFE membrane. Data were obtained in triplicate ( $n = 3$ ) and compared by *T*-test with a significance level of 5%.

## 2.6. TRAP staining

At 4 and 8 weeks, the harvested calvarias ( $n = 4$ ) were fixed in 10% buffered formalin (Merck, Germany) for 24 h, decalcified in buffered EDTA (Merck), dehydrated in ethanol, and embedded in paraffin (Merck). Five-micrometer thickness sections from central regions were stained with TRAP kit (Sigma-Aldrich, MO, USA) following the manufacturer's instructions. Then, the sections were counterstained with 1% light green (Merck). The images were obtained using light microscopy (Leica Microsystems Wetzlar GmbH, Germany) attached to a digital camera (DFC310 FX camera, Leica Microsystems). Positive TRAP staining was quantified in randomly acquired areas at 10 $\times$  magnification in quadruplicate ( $n = 4$ ), at 4 and 8 weeks. The TRAP-positive area was quantified by pixel count and expressed as a percentage of the total tissue area, using the Leica LAS Image Analysis Software (Leica Microsystem), and compared by ANOVA two-way test followed by Student–Newman–Keuls test with a significance level of 5%.

## 3. Results

Among the 276 evaluated miRs, 65 miRs were higher ( $\geq 2$  fold) and 11 were lower ( $\leq 2$  fold) expressed at 4 weeks (Table 1) while 26 miRs were higher ( $\geq 2$  fold) and 37 were lower ( $\leq 2$  fold) expressed at 8 weeks (Table 2) in bone tissue grown on PVDF compared with PTFE membrane. Twelve miRs were commonly increased at 4 and 8 weeks: miR-1, -10a, -28, -34a, -133b, -145, -190a, -214, -322, -511, -541, and -874 (Tables 1 and 2, gray highlight). The microarray data were validated by real-time PCR, which confirmed the higher expression of miR-146b ( $p = 0.036$ ) at 4 weeks and miR-29b and -10a ( $p = 0.001$  for both) at 8 weeks in bone tissue grown on PVDF compared with PTFE membrane (Figure 1).

Among the common higher expressed miRs ( $\geq 2$  fold) in both time points, we focused on the RANKL-targeted miR-34a that was increased ( $p = 0.016$ ) in bone tissue grown on PVDF compared with PTFE membrane (Figure 2(A)). The higher expression of miR-34a was concomitant with the decrease of its target RANKL ( $p = 0.004$ , Figure 2(B)). Furthermore, several miR-34a potential targets, LEF1 ( $p = 0.002$ ), ENG ( $p = 0.001$ ), YY1 ( $p = 0.001$ ), SYT1 ( $p = 0.001$ ), and CSFR ( $p = 0.009$ ) were also decreased in bone tissue grown on PVDF compared with PTFE membrane (Figure 2(C)).

In order to confirm our molecular findings, osteoclast cells were detected in histological sections of the bone tissue grown on PVDF and PTFE membranes using TRAP staining (Figure 3(A)–(F)). The quantification indicated a higher TRAP-positive area in bone

**Table 1.** Increased ( $\geq 2$  fold) and decreased ( $\leq 2$  fold) miRs of cells derived from bone tissue grown on PVDF compared with PTFE at 4 weeks.

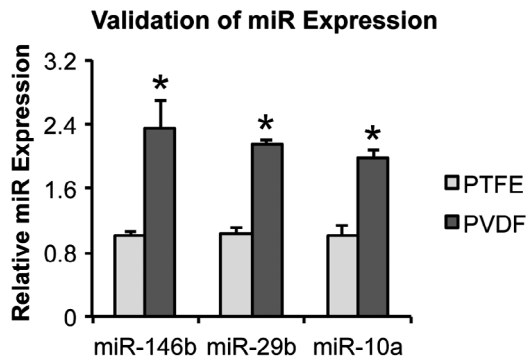
Increased miRs	Fold change	Decreased miRs	Fold change
133a	73.3	338	-7.0
1	39.8	181d	-3.0
206	9.0	182	-2.5
130a	6.5	144	-2.5
409a	6.0	31a	-2.0
341	5.0	99a	-2.0
34a	4.5	410	-2.0
133b	4.0	425	-2.0
137	4.0	504	-2.0
384	4.0	708	-2.0
434	4.0	1298	-2.0
210	3.7		
181c	3.5		
322	3.2		
19a	3.0		
24-2	3.0		
129	3.0		
134	3.0		
139	3.0		
152	3.0		
193	3.0		
221	3.0		
511	3.0		
541	3.0		
874	3.0		
146b	2.8		
211	2.7		
28	2.6		
351	2.6		
378a	2.6		
10a	2.5		
145	2.5		
374	2.5		
106b	2.0		
146a	2.4		
17	2.3		
127	2.3		
652	2.3		
125a	2.2		
125b	2.2		
3473	2.2		
30d	2.1		
450	2.1		
18a	2.0		
21	2.0		
106b	2.0		
125-1	2.0		
127	2.0		
143	2.0		
181c	2.0		
183	2.0		
190a	2.0		
214	2.0		
218a	2.0		
301a	2.0		
331	2.0		
376c	2.0		
378a	2.0		
384	2.0		
411	2.0		
485	2.0		
598	2.0		
872	2.0		
879	2.0		
3068	2.0		

Notes: Common increased miRs ( $\geq 2$  fold) at 4 and 8 weeks are highlighted in gray. Fold change compared with PTFE.

**Table 2.** Increased ( $\geq 2$  fold) and decreased ( $\leq 2$  fold) miRs of cells derived from bone tissue grown on PVDF compared with PTFE at 8 weeks.

Increased miRs	Fold change	Decreased miRs	Fold change
144	6.0	1298	-21.6
214	3.8	93	-12.0
10a	3.4	17	-11.0
423	3.3	182	-9.6
34a	3.0	223	-8.5
190a	3.0	204	-7.1
345	3.0	34c	-5.5
30c-2	3.0	30e	-5.3
29b	2.5	129-2	-5.0
133b	2.3	301a	-5.0
28	2.3	652	-4.5
99a	2.3	34b	-4.0
1	2.2	139	-4.0
145	2.0	598	-4.0
205	2.0	128	-3.5
322	2.0	132	-3.5
339	2.0	9a	-3.0
455	2.0	20b	-3.0
500	2.0	142	-3.0
501	2.0	219a	-3.0
504	2.0	335	-3.0
511	2.0	92a	-2.5
541	2.0	183	-2.5
542	2.0	211	-2.5
582	2.0	92b	-2.4
874	2.0	15b	-2.3
		18a	-2.0
		98	-2.0
		144	-2.0
		181d	-2.0
		497	-2.0
		106b	-2.0
		125b	-2.0
		187	-2.0
		361	-2.0
		409a	-2.0
		872	-2.0

Notes: Common increased miRs ( $\geq 2$  fold) at 4 and 8 weeks are highlighted in gray. Fold change compared with PTFE.

**Figure 1.** Expression of miR-146b at 4 weeks, and miR-29b and -10a at 8 weeks of bone tissue grown in rat calvarial defects implanted with polytetra-fluoroethylene (PTFE) or poly(vinylidene-trifluoroethylene)/barium titanate (PVDF) membrane.

Note: The data are presented as mean  $\pm$  standard deviation ( $n = 3$ ) and the asterisks indicate statistical significant difference between PTFE and PVDF ( $p \leq 0.05$ ).

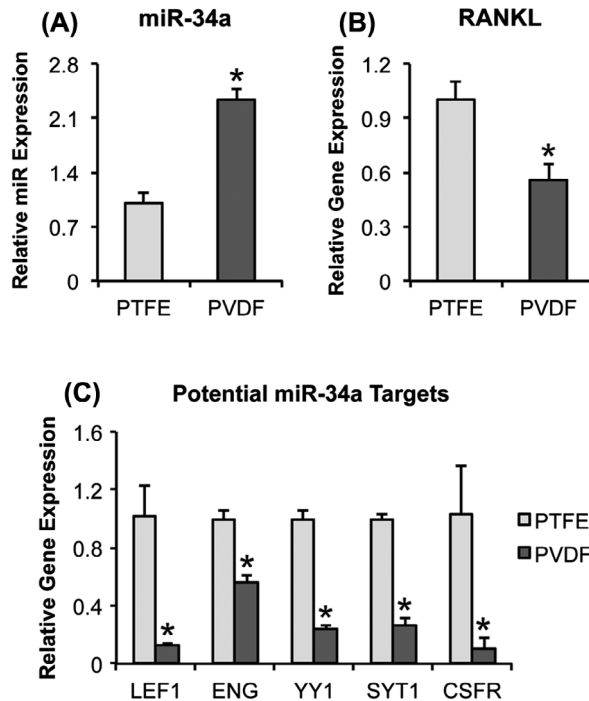


**Figure 2.** Expression of miR-34a (A), receptor activator of nuclear factor kappa-B ligand (RANKL; B), and lymphoid enhancer-binding factor 1 (LEF1), endoglin (ENG), YY1 transcription factor, synaptotagmin I (SYT1), and colony-stimulating factor 1 receptor (CSFR; C) at 8 weeks of bone tissue grown in rat calvarial defects implanted with polytetra-fluoroethylene (PTFE) or poly(vinylidene-trifluoroethylene)/barium titanate (PVDF) membrane.

Note: The data are presented as mean  $\pm$  standard deviation ( $n = 3$ ) and the asterisks indicate statistical significant difference between PTFE and PVDF ( $p \leq 0.05$ ).

tissue grown on PTFE compared with PVDF at both time points (Figure 3(G),  $p = 0.001$ ). Additionally, while no difference ( $p > 0.05$ ) was observed in TRAP-positive area in bone tissue grown on PVDF from 4 to 8 weeks, it increased in bone tissue grown on PTFE (Figure 3(G),  $p = 0.031$ ).

#### 4. Discussion

To date is well known the good *in vitro* and *in vivo* osteogenic potential of the PVDF membrane.[10–13] Here, we have shown that PVDF could also increase the process of bone repair by decreasing osteoclast differentiation and activity. As the expression of miR-34a was higher concomitantly with the lower expression of its target RANKL on PVDF compared with PTFE, we suggest that the enhanced bone formation induced by PVDF membrane is, at least in part, due to an imbalance in bone resorption mediated by a miR-34a/RANKL circuit.

In order to investigate mechanisms that could be implicated in the higher bone formation induced by PVDF membrane, we performed a large-scale analysis of the expression of miRs due to their important roles in the process of osteogenesis.[26–28] Among more than 250 miRs evaluated in bone tissue grown on membranes at 4 and 8 weeks, 12 miRs



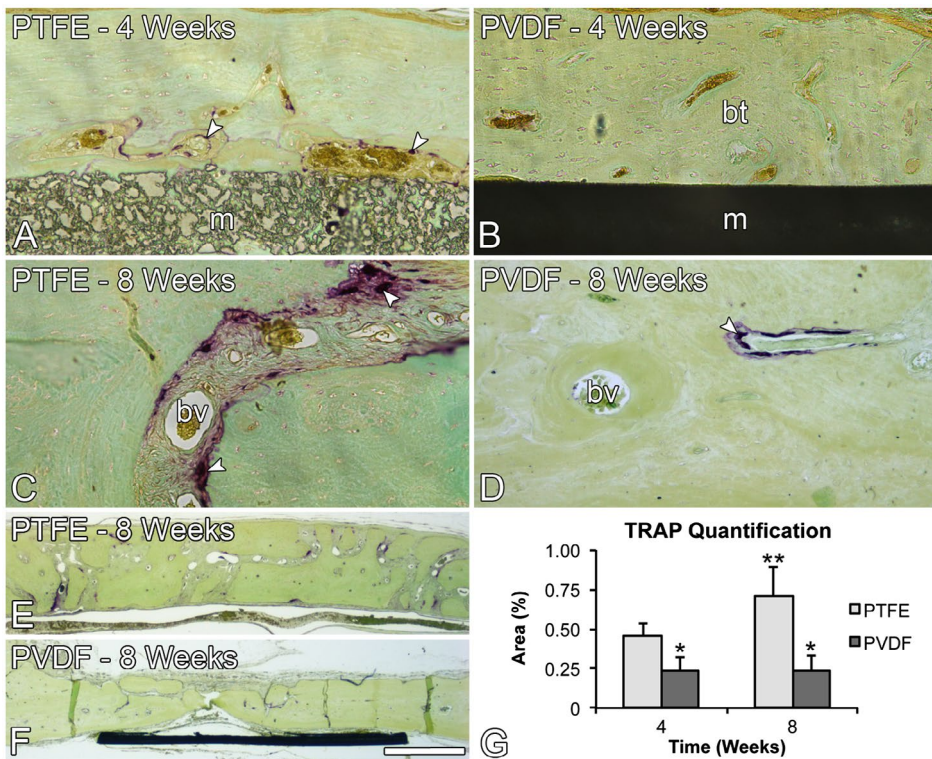


**Figure 3.** Light microscopy of rat calvarial bone defects implanted with polytetra-fluoroethylene (PTFE; A, C and E) or poly(vinylidene-trifluoroethylene)/ barium titanate (PVDF; B, D and F) membrane at 4 (A and B) and 8 (C–F) weeks stained with tartrate-resistant acid phosphatase (TRAP) and counterstained with 1% light green. The bone tissue grown on PTFE (A, C and E) exhibited more TRAP-positive cells (arrowheads) compared with PVDF (B, D and F) membrane as indicated by quantification (G).

Notes: The data (G) are presented as mean  $\pm$  standard deviation ( $n = 4$ ). One asterisk indicates statistical significant difference between PTFE and PVDF at the same time point and two asterisks indicates statistical significant difference between the time points ( $p \leq 0.05$ ). bt: bone tissue; bv: blood vessel; ct: connective tissue; m: membrane. Scale bar: A–D = 100  $\mu\text{m}$  and E–F = 800  $\mu\text{m}$ .

were higher expressed on PVDF compared with PTFE at both time points, including miR-34a. As miR-34a-target interactions are involved in some osteogenic signaling pathways, we focused our investigation on this miR.[29–31]

The miR-34a has been described as a physiologically relevant regulator of bone resorption that acts as a key suppressor of osteoclast development, leading to an increase in the total bone mass.[24] In keeping with this, we observed a higher expression of miR-34a along with a lower expression of RANKL, one of its targets, which plays a critical role in the osteoclastogenesis and bone remodeling processes, on PVDF compared with PTFE.[15] To confirm the biological relevance and effectiveness of the higher expression of miR-34a on PVDF, we evaluated several potential miR-34a target genes in the osteoclast lineage, LEF1, ENG, YY1, SYT1, and CSFR, and, as expected, they were all reduced in bone tissue grown on PVDF compared with PTFE membrane.[24] It is possible to suggest that this molecular finding may be directly related to an impairment in osteoclast differentiation and/or activity induced by PVDF, which thereby could be one of the mechanisms involved



in the higher amount of bone repair observed on this membrane compared with PTFE.[13] However, considering the limitations of our work, further studies are necessary to elucidate the participation of this RANKL-miR-34a circuit in the process of bone remodeling. In order to try to link the molecular events with the increased amount of bone, the presence of osteoclasts was evaluated and indeed we noticed a reduced number of TRAP-positive cells in the bone tissue grown on PVDF compared with PTFE membrane, suggesting the inhibitory effect of PVDF on osteoclastogenesis. In this context, this membrane could be a good alternative to be employed in clinical situations involving bone disorders where the process of resorption is exacerbated, such as osteoporosis.

In conclusion, we have shown that PVDF membrane regulates the expression of several miRs and some of them could be involved in the interactions of bone cells and biomaterials. Furthermore, our results suggest that PVDF membrane could induce higher bone repair, at least in part, by triggering an intracellular mechanism of increasing miR-34a/decreasing RANKL loop, which may inhibit osteoclast differentiation and/or activity, and bone resorption. In this context, our findings could represent a first step for developing biomaterials that directly modulate cell-signaling pathways implicated in both bone resorption and formation in order to promote bone regeneration.

## Acknowledgments

Dimitrius L. Pitol, Fabíola S. de Oliveira, Milla S. Tavares, and Roger R. Fernandes are acknowledged for technical assistance during the experiments. We also acknowledge Professor Mohammad Q. Hassan from UAB School of Dentistry for assistance with the experimental design and data analysis, and Michael R. Crowley and David K. Crossman from UAB Heflin Centre for Genomic Sciences for RNA sequencing analyses.

## Disclosure statement

The Authors declares that there is no conflict of interest.

## Funding

This work was supported by State of São Paulo Research Foundation (FAPESP, Brazil) [grant number 2011/10658-8], [grant number 2011/13623-0], [grant number 2013/01622-5] and Minas Gerais State Research Foundation (FAPEMIG, Brazil) [grant number TEC - APQ-03013-15].

## ORCID

Marcio M. Beloti  <http://orcid.org/0000-0003-0149-7189>

## References

- [1] Hämmerle CH, Jung RE. Bone augmentation by means of barrier membranes. *Periodontol.* 2000. **2003**;33:36–53.
- [2] Dimitriou R, Mataliotakis GI, Calori GM, et al. The role of barrier membranes for guided bone regeneration and restoration of large bone defects: current experimental and clinical evidence. *BMC Med.* **2012**;10:81.

- [3] Sanz-Sanchez I, Ortiz-Vigon A, Sanz-Martin I, et al. Effectiveness of lateral bone augmentation on the alveolar crest dimension: a systematic review and meta-analysis. *J. Dent. Res.* **2015**;94(9Suppl):128S–142S.
- [4] Jovanovic SA, Nevins M. Bone formation utilizing titanium-reinforced barrier membranes. *Int. J. Periodontics Restorative Dent.* **1995**;15:56–69.
- [5] Li J, Man Y, Zuo Y, et al. In vitro and in vivo evaluation of a nHA/PA66 composite membrane for guided bone regeneration. *J. Biomater. Sci. Polym. Ed.* **2011**;22:263–275.
- [6] Jung RE, Hälgl GA, Thoma DS, et al. A randomized, controlled clinical trial to evaluate a new membrane for guided bone regeneration around dental implants. *Clin. Oral Implant Res.* **2009**;20:162–168.
- [7] Matsumoto G, Hoshino J, Kinoshita Y, et al. Evaluation of guided bone regeneration with poly(lactic acid-co-glycolic acid-co-ε-caprolactone) porous membrane in lateral bone defects of the canine mandible. *Int. J. Oral Maxillofac. Implants.* **2012**;27:587–594.
- [8] Rowe MJ, Kamocki K, Pankajakshan D, et al. Dimensionally stable and bioactive membrane for guided bone regeneration: an in vitro study. *J. Biomed. Mater. Res. B Appl. Biomater.* **2016**;104:594–605. doi:<http://dx.doi.org/10.1002/jbm.b.33430>.
- [9] Gimenes R, Zaghete MA, Bertolini M, et al. Composites PVDF-TrFE/BT used as bioactive membranes for enhancing bone regeneration. In: Bar-Cohen Y, editor. *Proceedings of SPIE. Vol. 5385, Smart structures and materials.* Bellingham, WA: SPIE; **2004**. p. 539–547.
- [10] Beloti MM, de Oliveira PT, Gimenes R, et al. In vitro biocompatibility of a novel membrane of the composite poly(vinylidene-trifluoroethylene)/barium titanate. *J. Biomed. Mater. Res. A.* **2006**;79:282–288.
- [11] Teixeira LN, Crippa GE, Trabuco AC, et al. In vitro biocompatibility of poly(vinylidene fluoride-trifluoroethylene)/barium titanate composite using cultures of human periodontal ligament fibroblasts and keratinocytes. *Acta Biomater.* **2010**;6:979–989.
- [12] Teixeira LN, Crippa GE, Gimenes R, et al. Response of human alveolar bone-derived cells to a novel poly(vinylidene fluoride-trifluoroethylene)/barium titanate membrane. *J. Mater. Sci. Mater. Med.* **2011**;22:151–158.
- [13] Lopes HB, Santos TD, de Oliveira FS, et al. Poly(vinylidene-trifluoroethylene)/barium titanate composite for in vivo support of bone formation. *J. Biomater. Appl.* **2014**;29:104–112.
- [14] Yasuda H, Shima N, Nakagawa N, et al. Osteoclast differentiation factor is a ligand for osteoprotegerin/osteoclastogenesis-inhibitory factor and is identical to TRANCE/RANKL. *Proc. Natl. Acad. Sci. U. S. A.* **1998**;95:3597–3602.
- [15] Udagawa N, Takahashi N, Jimi E, et al. Osteoblasts/stromal cells stimulate osteoclast activation through expression of osteoclast differentiation factor/RANKL but not macrophage colony-stimulating factor: receptor activator of NF-κB ligand. *Bone.* **1999**;25:517–523.
- [16] Bartel DP. MicroRNAs: genomics, biogenesis, mechanism, and function. *Cell.* **2004**;116:281–297.
- [17] Mizuno Y, Tokuzawa Y, Ninomiya Y, et al. miR-210 promotes osteoblastic differentiation through inhibition of AcvR1b. *FEBS Lett.* **2009**;583:2263–2268.
- [18] Itoh T, Nozawa Y, Akao Y. MicroRNA-141 and -200a are involved in bone morphogenetic protein-2-induced mouse pre-osteoblast differentiation by targeting distal-less homeobox 5. *J. Biol. Chem.* **2009**;284:19272–19279.
- [19] Li Z, Hassan MQ, Jafferji M, et al. Biological functions of miR-29b contribute to positive regulation of osteoblast differentiation. *J. Biol. Chem.* **2009**;284:15676–15684.
- [20] Zhang J, Zhao H, Chen J, et al. Interferon-β-induced miR-155 inhibits osteoclast differentiation by targeting SOCS1 and MITF. *FEBS Lett.* **2012**;586:3255–3262.
- [21] Cheng P, Chen C, He HB, et al. MiR-148a regulates osteoclastogenesis by targeting V-maf musculoaponeurotic fibrosarcoma oncogene homolog B. *J. Bone Miner. Res.* **2013**;28:1180–1190.
- [22] Lee Y, Kim HJ, Park CK, et al. MicroRNA-124 regulates osteoclast differentiation. *Bone.* **2013**;56:383–389.

- [23] Rossi M, Pitari MR, Amodio N, et al. MiR-29b negatively regulates human osteoclastic cell differentiation and function: implications for the treatment of multiple myeloma-related bone disease. *J. Cell. Physiol.* **2013**;228:1506–1515.
- [24] Krzeszinski JY, Wei W, Huynh H, et al. miR-34a blocks osteoporosis and bone metastasis by inhibiting osteoclastogenesis and Tgif2. *Nature.* **2014**;28:431–435.
- [25] Santos T de S, Abuna RP, Almeida AL, et al. Effect of collagen sponge and fibrin glue on bone repair. *J. Appl. Oral Sci.* **2015**;23:623–628.
- [26] Hassan MQ, Tye CE, Stein GS, et al. Non-coding RNAs: epigenetic regulators of bone development and homeostasis. *Bone.* **2015**;81:746–756.
- [27] Qadir AS, Um S, Lee H, et al. miR-124 negatively regulates osteogenic differentiation and in vivo bone formation of mesenchymal stem cells. *J. Cell. Biochem.* **2015**;116:730–742.
- [28] Xie Q, Wang Z, Zhou H, et al. The role of miR-135-modified adipose-derived mesenchymal stem cells in bone regeneration. *Biomaterials.* **2016**;75:279–294.
- [29] Wei J, Shi Y, Zheng L, et al. miR-34s inhibit osteoblast proliferation and differentiation in the mouse by targeting SATB2. *J. Cell Biol.* **2012**;197:509–521.
- [30] Sun F, Wan M, Xu X, et al. Crosstalk between miR-34a and Notch signaling promotes differentiation in apical papilla stem cells (SCAPs) Crosstalk between miR-34a and notch signaling promotes differentiation in Apical Papilla Stem Cells (SCAPs). *J. Dent. Res.* **2014**;93:589–595.
- [31] Avtanski DB. Honokiol abrogates leptin-induced tumor progression by inhibiting Wnt1-MTA1- $\beta$ -catenin signaling axis in a microRNA-34a dependent manner. *Oncotarget.* **2015**;6:16396–16410.

Copyright of Journal of Biomaterials Science -- Polymer Edition is the property of Taylor & Francis Ltd and its content may not be copied or emailed to multiple sites or posted to a listserv without the copyright holder's express written permission. However, users may print, download, or email articles for individual use.